Chaos ARTICLE scitation.org/journal/cha

Soliton ratchet induced by random transitions among symmetric sine-Gordon potentials

Cite as: Chaos **29**, 053119 (2019); doi: 10.1063/1.5092797
Submitted: 14 February 2019 · Accepted: 29 April 2019 ·
Published Online: 20 May 2019

Jesús Casado-Pascual,[1,a)] Bernardo Sánchez-Rey,[2,b)] and Niurka R. Quintero[2,c)]

AFFILIATIONS

[1]Física Teórica, Universidad de Sevilla, Apartado de Correos 1065, 41080 Sevilla, Spain
[2]Departamento de Física Aplicada I, E.P.S., Universidad de Sevilla, Virgen de África 7, 41011 Sevilla, Spain

[a)]**Electronic mail:** jcasado@us.es
[b)]**Electronic mail:** bernardo@us.es
[c)]**Electronic mail:** niurka@us.es. **Also at:** Instituto Carlos I de Física Teórica y Computacional, Universidad de Granada, 18071 Granada, Spain.

ABSTRACT

The generation of net soliton motion induced by random transitions among N symmetric phase-shifted sine-Gordon potentials is investigated, in the absence of any external force and without any thermal noise. The phase shifts of the potentials and the damping coefficients depend on a stationary Markov process. Necessary conditions for the existence of transport are obtained by an exhaustive study of the symmetries of the stochastic system and of the soliton velocity. It is shown that transport is generated by unequal transfer rates among the phase-shifted potentials or by unequal friction coefficients or by a properly devised combination of potentials ($N > 2$). Net motion and inversions of the currents, predicted by the symmetry analysis, are observed in simulations as well as in the solutions of a collective coordinate theory. A model with high efficient soliton motion is designed by using multistate phase-shifted potentials and by breaking the symmetries with unequal transfer rates.

The directed transport of particles and solitons in the absence of net forces is termed the ratchet phenomenon. It appears in nonequilibrium systems when the spatial and/or temporal symmetries are broken. Generally, an asymmetric potential breaks the spatial symmetry and a biharmonic external force is used to break temporal ones. Symmetry considerations allow predicting the necessary conditions satisfied by potentials and forces in order to induce net motion. Moreover, the symmetry analysis reveals that the ratchet phenomenon also may occur when symmetric potentials are employed and no net forces are applied. In this paper, a stochastic soliton ratchet is investigated by using random transitions among N phase-shifted symmetric sine-Gordon potentials with no external forces and no thermal noise. A rigorous symmetry analysis carried out shows all the possibilities to induce current. Since our results may be related with experiments in Josephson junctions, a high efficient stochastic soliton ratchet is designed by using multistate phase-shifted potentials and by breaking the symmetries with unequal transfer rates.

I. INTRODUCTION

Ratchet phenomenon of particles appears in nonequilibrium systems when the relevant symmetries are broken.[1] While spatial inversion symmetries are broken by means of asymmetric potentials,[2] the noise sources jointly with external forces guarantee the nonequilibrium.[3] *Soliton ratchet*, the natural extension of this phenomenon to complex nonlinear objects,[4,5] such as fluxons[6–9] and chains of colloidal particles,[10] has attracted a lot of attention in recent years due to its potential practical applications.[11,12]

The ratchet effect of particles and solitons is governed by the symmetries of the systems.[13,14] In the experimental realizations, even if the physical models are unknown, there are measurements which depend only on the symmetry properties of the magnitudes and devices.[7,9,15–17] The presence of certain symmetries leads us to predict the specific conditions for the absence of net motion and its inversion upon the variation of system parameters.[1,18] Moreover, when harmonic forces or potentials are used to induce the effect, symmetry considerations alone predict the current dependence on the

phases and amplitudes of all harmonics, regardless of the system under consideration.[13,14]

Symmetries predict the existence of soliton ratchets in deterministic models, where the time and space average of all external forces is zero. The mechanism leading to a net soliton motion is the desymmetrization of the basins of attraction that correspond to solitons moving in opposite directions. This is basically achieved through different combinations of asymmetric field potentials and/or asymmetric external ac forces (see Refs. 19–22 as well as the review article[23]). Curiously, from the analysis of symmetries, it turns out that the asymmetries of the potential and of the time-dependent external forces are not essential.[24,25] Indeed, in Ref. 25, a biased drift of soliton was achieved, in the absence of any external force, by a simple combination of two symmetric potentials with a relative phase-shift and deterministic transitions between them at fixed times.

Originally, the ratchet phenomenon was proposed as the possibility of rectifying thermal fluctuations of particles.[26–31] The findings of these studies motivated the examination of solitons in noisy environments.[32,33] Under the influence of white noise, the robustness of the soliton transport was numerically established[4,34,35] and the study of the whole phase-space of the system was enhanced.[36] It is worth mentioning that the sole action of the time-correlated noise sources was unable to induce any net motion of solitons,[32,33] although the inclusion of noise effectively added a unidirectional motion in a parameter range where zero-averaged velocity was observed for deterministic cases.[21,37,38] In spite of all these studies, the rigorous analysis of the symmetries in the context of stochastic soliton ratchets remains unaddressed.

Therefore, the main purpose of the current research is to explore in depth the symmetries of stochastic soliton ratchets. As a paradigmatic model, we focus on the damped sine-Gordon (sG) equation, in which random transitions occur among phase-shifted symmetric potentials, each of them having its own dissipation. Symmetries dictate that in a single symmetric potential, it would be impossible to obtain a directed soliton motion. It is only the random transitions among these potentials that are rectified, giving rise to a net current. Remarkably, a detailed study of the symmetries of the system reveals that there are several ways to reach net movement. Perhaps the most evident is by using unequal transfer rates. But other possibilities, such as unequal frictions and proper combinations of phase shifts, are also investigated. This stochastic route to soliton ratchet has already been studied for Brownian particles,[39–42] where the inter-potential transfers coexist with the thermal noise, thereby adding an extra source of randomness to the dynamics. However, in our study, neither thermal noise nor external forces are present. The rectification mechanism emerges through the coupling between the transfer rates and the internal structure of the soliton. This is clarified using a collective coordinate (CC) theory that provides a better understanding of the simulation results and complements the symmetry analysis. All this investigation leads us to address a second goal: the design of an efficient soliton ratchet, that is, a directed soliton motion with high average velocity. This is achieved by tuning the random fluctuations among N symmetric sG potentials so that the resulting phase shift always increases.

The outline of the paper is as follows. In Sec. II, a damped sG system with random transitions among a set of phase-shifted symmetric potentials is introduced, and a thorough analysis of the symmetries present is provided. Numerical simulations that verify the existence of the soliton ratchet phenomenon are presented in Sec. III. Different ways of breaking the symmetry and comparison with the CC approximation are explored. In Sec. IV, a multistate case is proposed that is properly designed in order to attain a very efficient rectification mechanism. Finally, our main results are summarized in the conclusions.

II. MODEL AND SYMMETRY CONSIDERATIONS

In the present study, we consider a sine-Gordon equation of the form

$$\partial_{tt}\Phi(x,t) - \partial_{xx}\Phi(x,t) = -\beta_{J(t)}\partial_t\Phi(x,t) - \sin\left[\Phi(x,t) + \theta_{J(t)}\right], \tag{1}$$

where both the damping coefficient $\beta_{J(t)}$ and the phase-shift $\theta_{J(t)}$ depend on a stationary Markovian stochastic process $J(t)$, which takes values in a set of N possible states $\{1,\ldots,N\}$. Thus, Eq. (1) represents a sG system in which random transitions occur among phase-shifted symmetric potentials, $U_{J(t)} = 1 - \cos[\Phi(x,t) + \theta_{J(t)}]$, each of which has its own dissipation. This type of equation has been used to model the dynamics of the phase difference Φ of Josephson junctions with tunable phase shifts $\theta_{J(t)}$.[12,43–45]

A more general situation in which the fluctuations of β and θ are governed by different stochastic processes $H(t)$ and $K(t)$, respectively, could also have been considered. However, it can be shown that this case can alternatively be described using only a single stochastic process, with a number of states equal to the product of the number of states of $H(t)$ and $K(t)$, and whose statistical properties are determined from those of $H(t)$ and $K(t)$.

The Markovian process $J(t)$ is fully determined by the probability p_j for $J(t)$ to take the value j at any time instant, and by the conditional probability $p(j,t|k,0)$ for $J(t)$ to take the value j at t, given that its value at 0 is k. Both p_j and $p(j,t|k,0)$ satisfy a master equation of the form

$$\partial_t P_j(t) = \sum_{j'=1}^{N} W_{j,j'} P_{j'}(t), \tag{2}$$

with $W_{j,j'} = w_{j,j'} - \delta_{j,j'}\sum_{j''=1}^{N} w_{j'',j}$, where $w_{j,j'}$ is the transition probability per unit time from state j' to state j. Specifically, p_j is a normalized time-independent solution of Eq. (2) and $p(j,t|k,0)$ is the solution of Eq. (2) corresponding to the initial condition $P_j(0) = \delta_{j,k}$. For simplicity, it will henceforth be assumed that there exists only one normalized time-independent solution of Eq. (2), so that $J(t)$ is uniquely determined by the transition matrix $\mathbb{W}$ with entries $W_{j,j'}$.

Since our focus is on solutions of Eq. (1) with only one kinklike structure present, boundary conditions of the forms

$$\lim_{x\to+\infty}\Phi(x,t) = \lim_{x\to-\infty}\Phi(x,t) + 2\pi \tag{3}$$

and

$$\lim_{x\to+\infty}\partial_x\Phi(x,t) = \lim_{x\to-\infty}\partial_x\Phi(x,t) \tag{4}$$

are considered. In addition, kinklike functions of the forms

$$\Phi(x,0) = 4\arctan(e^x) - \bar{\theta} \tag{5}$$

and

$$\partial_t \Phi(x,0) = 0 \tag{6}$$

are used as initial conditions, where $\bar{\theta} = \sum_{j=1}^{N} \theta_j/N$ is the arithmetic average of the phase shifts.

Let $\Phi\left[x,t;\boldsymbol{\theta},\boldsymbol{\beta},j(\cdot)\right]$ denote the solution of Eq. (1) corresponding to a particular realization $j(\cdot)$ of the aforementioned stochastic process. In order to determine the symmetry properties, the dependence on the parameters appearing in Eq. (1) has been explicitly indicated by introducing the column vectors $\boldsymbol{\theta} = (\theta_1,\ldots,\theta_N)^T$ and $\boldsymbol{\beta} = (\beta_1,\ldots,\beta_N)^T$. The velocity of the kink and the average kink velocity can be, respectively, calculated from the expressions

$$V\left[t;\boldsymbol{\theta},\boldsymbol{\beta},j(\cdot)\right] = \frac{1}{2\pi}\int_{-\infty}^{+\infty} dx\, x\partial_{tx}\Phi\left[x,t;\boldsymbol{\theta},\boldsymbol{\beta},j(\cdot)\right] \tag{7}$$

and

$$\overline{V}(t;\boldsymbol{\theta},\boldsymbol{\beta},\mathbb{W}) = \langle V\left[t;\boldsymbol{\theta},\boldsymbol{\beta},j(\cdot)\right]\rangle_{\mathbb{W}}, \tag{8}$$

where $\langle\cdot\rangle_{\mathbb{W}}$ denotes the average over the realizations of the process $J(t)$ corresponding to a given transition matrix $\mathbb{W}$. Finally, the long-time average velocity is given by the limit

$$\overline{V}_{\infty}(\boldsymbol{\theta},\boldsymbol{\beta},\mathbb{W}) = \lim_{t\to\infty}\overline{V}(t;\boldsymbol{\theta},\boldsymbol{\beta},\mathbb{W}). \tag{9}$$

For an arbitrary value $\Delta\theta$, let us consider the vector $\boldsymbol{\Delta\theta} = (\Delta\theta,\ldots,\Delta\theta)^T$. Then, it is easy to verify that the function $\Phi\left[x,t;\boldsymbol{\theta}+\boldsymbol{\Delta\theta},\boldsymbol{\beta},j(\cdot)\right] + \Delta\theta$ satisfies the problem given by Eqs. (1) and (3)–(6). Therefore, from the uniqueness of the solution of this problem, it follows that $\Phi\left[x,t;\boldsymbol{\theta},\boldsymbol{\beta},j(\cdot)\right] = \Phi\left[x,t;\boldsymbol{\theta}+\boldsymbol{\Delta\theta},\boldsymbol{\beta},j(\cdot)\right] + \Delta\theta$. By using Eqs. (7), (8), and (9), one then obtains that

$$V\left[t;\boldsymbol{\theta},\boldsymbol{\beta},j(\cdot)\right] = V\left[t;\boldsymbol{\theta}+\boldsymbol{\Delta\theta},\boldsymbol{\beta},j(\cdot)\right], \tag{10}$$

$$\overline{V}\left(t;\boldsymbol{\theta},\boldsymbol{\beta},\mathbb{W}\right) = \overline{V}\left(t;\boldsymbol{\theta}+\boldsymbol{\Delta\theta},\boldsymbol{\beta},\mathbb{W}\right), \tag{11}$$

and

$$\overline{V}_{\infty}\left(\boldsymbol{\theta},\boldsymbol{\beta},\mathbb{W}\right) = \overline{V}_{\infty}\left(\boldsymbol{\theta}+\boldsymbol{\Delta\theta},\boldsymbol{\beta},\mathbb{W}\right). \tag{12}$$

Analogously, it can be verified that the function $2\pi - 2\bar{\theta} - \Phi\left[-x,t;2\bar{\boldsymbol{\theta}}-\boldsymbol{\theta},\boldsymbol{\beta},j(\cdot)\right]$, with $\bar{\boldsymbol{\theta}} = (\bar{\theta},\ldots,\bar{\theta})^T$, also satisfies the problem given by Eqs. (1) and (3)–(6). Therefore, from the uniqueness of the solution of this problem, it follows that $\Phi\left[x,t;\boldsymbol{\theta},\boldsymbol{\beta},j(\cdot)\right] = 2\pi - 2\bar{\theta} - \Phi\left[-x,t;2\bar{\boldsymbol{\theta}}-\boldsymbol{\theta},\boldsymbol{\beta},j(\cdot)\right]$. Thus, using Eqs. (7), (8), and (9), it is straightforward to see that

$$V\left[t;\boldsymbol{\theta},\boldsymbol{\beta},j(\cdot)\right] = -V\left[t;2\bar{\boldsymbol{\theta}}-\boldsymbol{\theta},\boldsymbol{\beta},j(\cdot)\right], \tag{13}$$

$$\overline{V}\left(t;\boldsymbol{\theta},\boldsymbol{\beta},\mathbb{W}\right) = -\overline{V}\left(t;2\bar{\boldsymbol{\theta}}-\boldsymbol{\theta},\boldsymbol{\beta},\mathbb{W}\right), \tag{14}$$

and

$$\overline{V}_{\infty}\left(\boldsymbol{\theta},\boldsymbol{\beta},\mathbb{W}\right) = -\overline{V}_{\infty}\left(2\bar{\boldsymbol{\theta}}-\boldsymbol{\theta},\boldsymbol{\beta},\mathbb{W}\right). \tag{15}$$

A direct consequence of the three equations above, together with Eqs. (10), (11), and (12) for $\Delta\theta = -2\bar{\theta}$, is that

$$V\left[t;\boldsymbol{\theta},\boldsymbol{\beta},j(\cdot)\right] = -V\left[t;-\boldsymbol{\theta},\boldsymbol{\beta},j(\cdot)\right], \tag{16}$$

$$\overline{V}\left(t;\boldsymbol{\theta},\boldsymbol{\beta},\mathbb{W}\right) = -\overline{V}\left(t;-\boldsymbol{\theta},\boldsymbol{\beta},\mathbb{W}\right), \tag{17}$$

and

$$\overline{V}_{\infty}\left(\boldsymbol{\theta},\boldsymbol{\beta},\mathbb{W}\right) = -\overline{V}_{\infty}\left(-\boldsymbol{\theta},\boldsymbol{\beta},\mathbb{W}\right). \tag{18}$$

At this point, it is worth mentioning that the ordering that we have chosen for labeling the states of the stochastic process $J(t)$ is completely arbitrary and, therefore, modification of such ordering does not alter the physical results. This implies that $\overline{V}(t;\boldsymbol{\theta},\boldsymbol{\beta},\mathbb{W})$ and $\overline{V}_{\infty}(\boldsymbol{\theta},\boldsymbol{\beta},\mathbb{W})$ must be invariant under permutations of the labels assigned to the states of $J(t)$. In order to mathematically formulate this invariance, let us consider a permutation σ of the N states and define the $N\times N$ matrix $\mathbb{T}_\sigma$ with components $(\mathbb{T}_\sigma)_{jj'} = \delta_{\sigma j,j'}$, where σj is the result of applying the permutation σ to the state j. Then, the parameters $\{\boldsymbol{\theta},\boldsymbol{\beta},\mathbb{W}\}$ and $\left\{\mathbb{T}_\sigma\boldsymbol{\theta},\mathbb{T}_\sigma\boldsymbol{\beta},\mathbb{T}_\sigma\mathbb{W}\mathbb{T}_\sigma^T\right\}$ represent essentially the same system and, consequently,

$$\overline{V}(t;\boldsymbol{\theta},\boldsymbol{\beta},\mathbb{W}) = \overline{V}(t;\mathbb{T}_\sigma\boldsymbol{\theta},\mathbb{T}_\sigma\boldsymbol{\beta},\mathbb{T}_\sigma\mathbb{W}\mathbb{T}_\sigma^T) \tag{19}$$

and

$$\overline{V}_{\infty}(\boldsymbol{\theta},\boldsymbol{\beta},\mathbb{W}) = \overline{V}_{\infty}(\mathbb{T}_\sigma\boldsymbol{\theta},\mathbb{T}_\sigma\boldsymbol{\beta},\mathbb{T}_\sigma\mathbb{W}\mathbb{T}_\sigma^T). \tag{20}$$

Let us assume now that there exists a permutation $\tilde{\sigma}$ such that $\mathbb{T}_{\tilde{\sigma}}\boldsymbol{\theta} = 2\bar{\boldsymbol{\theta}} - \boldsymbol{\theta}$. According to Eqs. (14) and (15), it is, therefore, clear that

$$\overline{V}\left(t;\boldsymbol{\theta},\boldsymbol{\beta},\mathbb{W}\right) = -\overline{V}\left(t;\mathbb{T}_{\tilde{\sigma}}\boldsymbol{\theta},\boldsymbol{\beta},\mathbb{W}\right) \tag{21}$$

and

$$\overline{V}_{\infty}\left(\boldsymbol{\theta},\boldsymbol{\beta},\mathbb{W}\right) = -\overline{V}_{\infty}\left(\mathbb{T}_{\tilde{\sigma}}\boldsymbol{\theta},\boldsymbol{\beta},\mathbb{W}\right). \tag{22}$$

Taking into account that $\mathbb{T}_{\tilde{\sigma}}\mathbb{T}_{\tilde{\sigma}}\boldsymbol{\theta} = \boldsymbol{\theta}$ and Eqs. (19), (20), (21), and (22), one then obtains that

$$\overline{V}\left(t;\boldsymbol{\theta},\boldsymbol{\beta},\mathbb{W}\right) = -\overline{V}\left(t;\boldsymbol{\theta},\mathbb{T}_{\tilde{\sigma}}\boldsymbol{\beta},\mathbb{T}_{\tilde{\sigma}}\mathbb{W}\mathbb{T}_{\tilde{\sigma}}^T\right) \tag{23}$$

and

$$\overline{V}_{\infty}\left(\boldsymbol{\theta},\boldsymbol{\beta},\mathbb{W}\right) = -\overline{V}_{\infty}\left(\boldsymbol{\theta},\mathbb{T}_{\tilde{\sigma}}\boldsymbol{\beta},\mathbb{T}_{\tilde{\sigma}}\mathbb{W}\mathbb{T}_{\tilde{\sigma}}^T\right). \tag{24}$$

From the above two equations, it is clear that if $\mathbb{T}_{\tilde{\sigma}}\boldsymbol{\beta} = \boldsymbol{\beta}$ and $\mathbb{T}_{\tilde{\sigma}}\mathbb{W}\mathbb{T}_{\tilde{\sigma}}^T = \mathbb{W}$, then $\overline{V}\left(t;\boldsymbol{\theta},\boldsymbol{\beta},\mathbb{W}\right) = \overline{V}_{\infty}\left(\boldsymbol{\theta},\boldsymbol{\beta},\mathbb{W}\right) = 0$. Consequently, a necessary condition for the existence of directed motion is that there exists no permutation $\tilde{\sigma}$ which simultaneously verifies

(i) $\mathbb{T}_{\tilde{\sigma}}\boldsymbol{\theta} = 2\bar{\boldsymbol{\theta}} - \boldsymbol{\theta}$,
(ii) $\mathbb{T}_{\tilde{\sigma}}\boldsymbol{\beta} = \boldsymbol{\beta}$, and
(iii) $\mathbb{T}_{\tilde{\sigma}}\mathbb{W}\mathbb{T}_{\tilde{\sigma}}^T = \mathbb{W}$.

A direct consequence of this result is that, as is to be expected, it is impossible to induce directed motion by only fluctuating the damping coefficients while keeping a fixed potential. Indeed, in this case, the identity permutation would satisfy the aforementioned conditions leading to the absence of average motion.

III. NUMERICAL STUDY OF THE SYMMETRIES

We have performed numerical simulations of the damped sG equation (1), with the boundary conditions (3) and (4) and initial conditions (5) and (6), in order to check the existence of net kink motion due to stochastic transitions among symmetric sG potentials. A Runge–Kutta algorithm with space step $\Delta x = 0.02$ and time step $\Delta t = 0.02$ has been used. A total number of 2500 points have been considered such that the length of the system is $L = 50$.

We have verified numerically that, for this system, averaging over realizations provides the same results as performing a time-average over a sufficiently long single trajectory. The latter procedure has been used in the numerical calculations owing to its better computational efficiency. In order to prevent spurious effects due to the finite size of the system, we have divided the kink trajectory into $M = 100$ time intervals of duration $T = 5000$ units of time, after which the whole system is shifted so that the kink center of mass is reset to zero. For each interval, the time-average velocity is computed as

$$V_i = \frac{1}{T}\int_{t_i}^{t_i+T} dt\, \partial_t X(t) = \frac{X(t_i+T) - X(t_i)}{T} \quad (i = 1, 2, \ldots, M), \tag{25}$$

where $t_i = (i-1)T$ and

$$X(t) = \frac{1}{2\pi}\int_{-\infty}^{+\infty} dx\, x\partial_x \Phi(x,t) \tag{26}$$

is the center of mass of the kink, in accordance with expression (7). Note that, as a consequence of the shift of the center of mass described above, $X(t_i) = 0$ for $i = 1, \ldots, M$ in Eq. (25). The long-time average velocity is then obtained as

$$\overline{V}_\infty = \frac{1}{M}\sum_{i=1}^{M} V_i. \tag{27}$$

As an example, let us first consider the simplest case of a two-state sG system. This means that $J(t)$ will only take two possible values 1 and 2 and, consequently, the set of symmetric potentials is reduced to two elements,

$$U_1(\Phi) = 1 - \cos(\Phi + \theta_1),$$
$$U_2(\Phi) = 1 - \cos(\Phi + \theta_2). \tag{28}$$

In this case, regardless of the values of θ_1 and θ_2, condition (i) of Sec. II always holds for the transposition $\tilde{\sigma}1 = 2$ and $\tilde{\sigma}2 = 1$, which corresponds to the matrix

$$\mathbb{T}_{\tilde{\sigma}} = \begin{bmatrix} 0 & 1 \\ 1 & 0 \end{bmatrix}. \tag{29}$$

Therefore, directed motion can be generated on the condition that $\beta_1 \neq \beta_2$ and/or $W_{1,2} \neq W_{2,1}$. In addition, according to Eq. (24), it is clear that

$$\overline{V}_\infty(\theta_1, \theta_2, \beta_1, \beta_2, W_{1,2}, W_{2,1}) = -\overline{V}_\infty(\theta_1, \theta_2, \beta_2, \beta_1, W_{2,1}, W_{1,2}). \tag{30}$$

For this dichotomous Markov process, the equilibrium population of the state j is

$$p_j = \frac{W_{jj'}}{W_{jj'} + W_{j'j}} \quad (j \neq j'), \tag{31}$$

and the residence time, τ_j, in the state j has a probability density

$$g(\tau_j) = W_{jj'} \exp(-W_{jj'}\tau_j) \quad (j \neq j'). \tag{32}$$

Consequently, a realization of the process $J(t)$ can be performed assigning to each state j residence time values

$$\tau_j = -\ln(z)/W_{jj'} \quad (j \neq j'), \tag{33}$$

where z is a random number between 0 and 1.

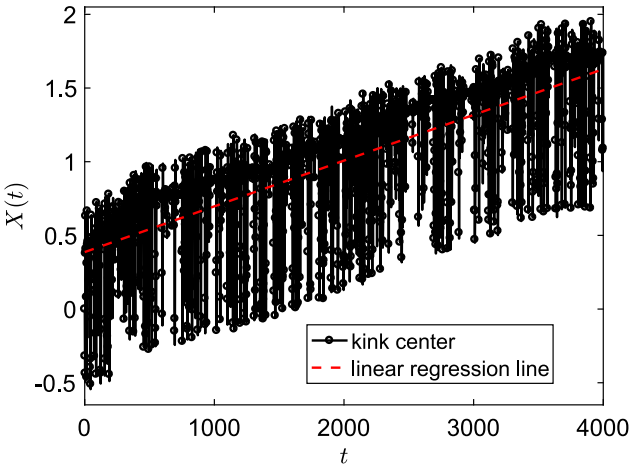

FIG. 1. Time evolution of the kink center for a dichotomous Markov process $J(t)$ with transition rates $W_{2,1} = 0.4$ and $W_{1,2} = 0.1$. The dashed straight line is the linear regression line that fits the data. Its slope provides a guide so that the net movement of the kink to the right can be appreciated. The remaining parameter values are $\beta_1 = \beta_2 = 0.8$ and $\theta_1 = -\theta_2 = 0.5$.

Let us initially take $\theta_1 = -\theta_2 = 0.5$ and $\beta_1 = \beta_2 = 0.8$. Directed motion is possible only if $W_{1,2} \neq W_{2,1}$. For $W_{2,1} = 0.4$ and $W_{1,2} = 0.1$, one realization of the time evolution of the kink center can be observed in Fig. 1. The dashed straight line is the linear regression line that fits the data. This line has been plotted only as a guide to the eye in order to appreciate the net movement of the kink to the right and, therefore, the appearance of a ratchet effect.

The dependence of the kink velocity on the asymmetry parameter $\Delta p = p_2 - p_1 = (W_{2,1} - W_{1,2})/(W_{1,2} + W_{2,1})$, for fixed $W_{1,2} + W_{2,1} = 0.5$, is shown in Fig. 2. The circles correspond to the simulation of the sG equation (1), while the line represents a CC approximation. This CC theory (very briefly described in the Appendix, and whose details can be found in Ref. 25) employs three collective coordinates: the kink center, its width, and the value of the background field, whose role is essential for the appearance of the ratchet effect. The phase difference between the potentials considered in Eq. (28) induces significative changes in the background which, via its coupling with the kink width, supplies momentum to the kink center [see Eq. (A2) in the Appendix]. Note also how the symmetry (30) for equal frictions, $\beta_2 = \beta_1$, can be clearly appreciated. Indeed, $\overline{V}_\infty$ is an odd function in Δp, and, moreover, $\overline{V}_\infty = 0$ for $\Delta p = 0$ (i.e., for equal transition rates). The lack of ratchet effect when $\Delta p = \pm 1$ corresponds to the limiting cases in which no transitions occur. As a consequence, $\overline{V}_\infty$ displays nonmonotonous behavior reaching extrema at $\Delta p \approx \pm 0.60$.

If we consider again a dichotomous Markov process $J(t)$ between the potential states specified in (28) but now with equal transfer rates, then the only possibility for the generation of a net motion is by breaking condition (ii) of Sec. II, that is, by choosing different frictions (see Refs. 40, 46, and 47, where the friction coefficients break the dynamical symmetry and generate net motion of particles). The resulting long-time average velocity is plotted in Fig. 3

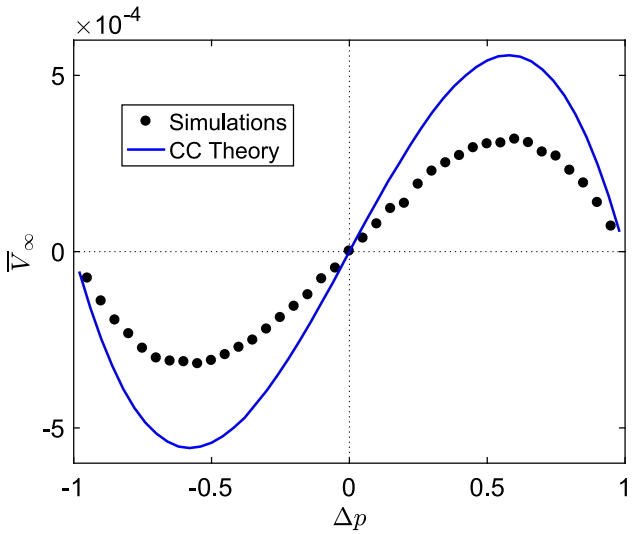

FIG. 2. Dependence of the averaged kink velocity on $\Delta p = p_2 - p_1$ for fixed $W_{1,2} + W_{2,1} = 0.5$ (circles). The result obtained by using the collective coordinate theory is depicted with a solid line. The remaining parameter values are $\beta_1 = \beta_2 = 0.8$ and $\theta_1 = -\theta_2 = 0.5$.

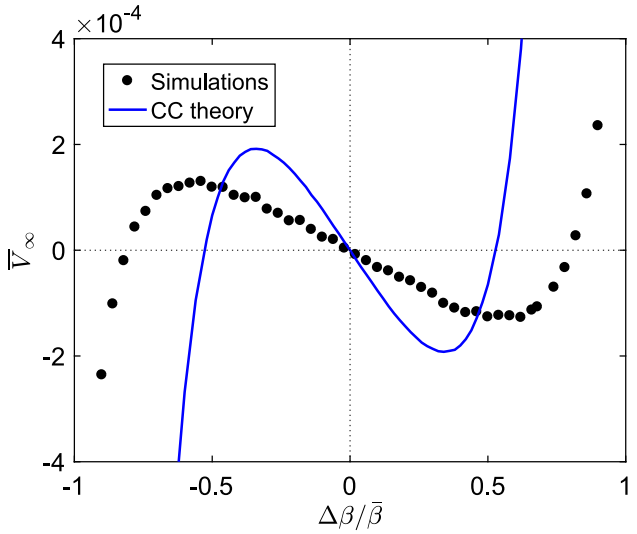

FIG. 3. Dependence of the averaged kink velocity on $\Delta\beta/\bar{\beta}$, where $\Delta\beta = \beta_2 - \beta_1$ and $\bar{\beta} = \beta_1 + \beta_2$, for a fixed value of $\bar{\beta} = 2$ (circles). The result obtained by using the collective coordinate theory is depicted with a solid line. The remaining parameter values are $W_{1,2} = W_{2,1} = 0.1$ and $\theta_1 = -\theta_2 = 0.5$.

as a function of $\Delta\beta/\bar{\beta}$, where $\Delta\beta = \beta_2 - \beta_1$ and $\bar{\beta} = \beta_1 + \beta_2$, for a fixed value of $\bar{\beta} = 2$ (circles). The CC theory (solid line) provides only a qualitative description of the simulation results. Both CC theory and simulation show clearly two consequences of the symmetry (30) for equal transfer rates $W_{1,2} = W_{2,1}$: zero averaged kink velocity for $\Delta\beta = 0$ ($\beta_1 = \beta_2$) and the fact that $\overline{V}_\infty$ is an odd function of $\Delta\beta$. Moreover, current reversals are observed. This is a counterintuitive effect, namely, that by varying the damping the direction of the current can be reversed.[47] The subsequent fast increase (decrease) of the kink velocity corresponds to the limit $\Delta\beta/\bar{\beta} \to +1(-1)$ in which the friction of one of the two states tends toward zero. In this limit, the kink becomes unstable and is eventually destroyed by the transitions. For this reason, we have restricted the simulations to the interval $-0.9 \leq \Delta\beta/\bar{\beta} \leq 0.9$.

Let us consider finally a third case in which symmetry conditions (ii) and (iii) of Sec. II are fulfilled but condition (i) is broken. In order to break (i), at least three states are necessary. Therefore, to the states specified in (28), let us add a third state

$$U_3(\Phi) = 1 - \cos(\Phi + \theta_3) \tag{34}$$

and keep $\theta_1 = -\theta_2 = 0.5$. Even if equal frictions for the three states and equal transfer rates between them are chosen, directed motion may in principle be generated except for $\theta_3 = 0$ and $\theta_3 = \pm 3/2$, since for any permutation σ, $\theta_{\sigma 3} \neq 2\bar{\theta} - \theta_3 = -\theta_3/3$.

The resulting kink velocities as functions of θ_3 are shown in Fig. 4. We have restricted θ_3 to the range $-0.5 \leq \theta_3 \leq 0.5$ in order to avoid transitions between states with phase differences larger than 1, which generate strong deformations in the kink structure. The CC theory (solid line) reasonably approaches the simulation results (circles). Notice that $\overline{V}_\infty$ is an odd function of θ_3. This property can be easily understood by taking into account Eq. (18) together with Eq. (20) for the permutation $\sigma 1 = 2$, $\sigma 2 = 1$ and $\sigma 3 = 3$, which corresponds to the matrix

$$\mathbb{T}_\sigma = \begin{bmatrix} 0 & 1 & 0 \\ 1 & 0 & 0 \\ 0 & 0 & 1 \end{bmatrix}. \tag{35}$$

IV. HIGH EFFICIENT RATCHET

In Sec. III, the net motion is achieved in successive stages, where the kink advances and backs up asymmetrically as shown in Fig. 1. For this reason, similarly to other soliton ratchets,[4,19,25,34] the averaged kink velocities obtained are rather low. In this respect, the improvement of the efficiency of the ratchet phenomenon has attracted the attention of experimentalists and theoreticians in the context of Josephson junctions.[8,48]

Here, in order to enhance the efficiency of the ratchet effect, a new case in which $J(t)$ is now a Poisson process is considered. This process takes values j in a set $\{1, \ldots, N\}$, and the corresponding phase shifts are $\theta_j = -2\pi j/N$. Initially, $J(0) = 1$ and its value increases in time with steps of one unit that occur at random moments with a rate $W_{j+1,j} = \gamma$. The label j is periodic because after the value N, it then again takes the value 1. In other words, $W_{j,j'} = \gamma\delta_{j,j'+1}$ for $j' \in \{1, \ldots, N-1\}$ and $W_{j,N} = \gamma\delta_{j,1}$. Moreover, we will take equal frictions $\beta_j = 0.8$, for $j = 1, \ldots, N$. Therefore, a realization of this process is a sequence of random jumps from the potential

$$U_j(\Phi) = 1 - \cos\left(\Phi - \frac{2\pi j}{N}\right) \tag{36}$$

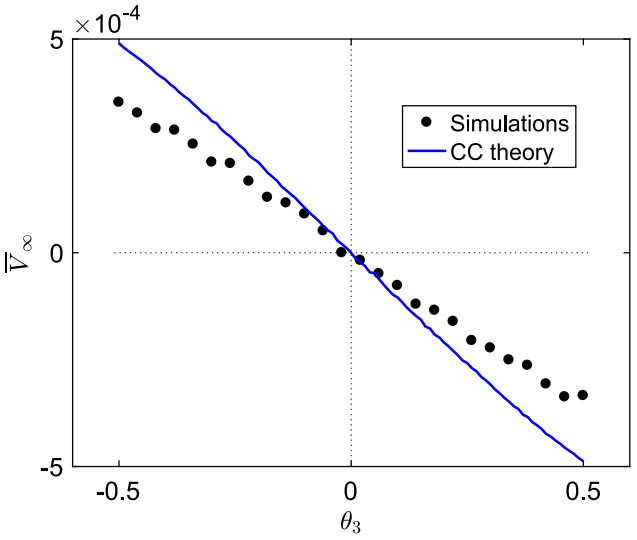

FIG. 4. Dependence of the averaged kink velocity on θ_3 for fixed $\theta_1 = -\theta_2 = 0.5$ (circles). The result obtained by using the collective coordinate theory is depicted with a solid line. The remaining parameter values are $W_{j,j'} = 0.5$, for all $j \neq j'$, and $\beta_1 = \beta_2 = \beta_3 = 0.8$.

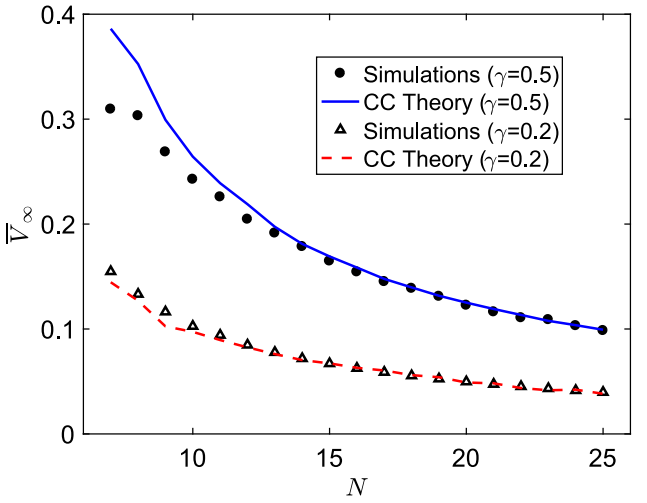

FIG. 5. Dependence of the averaged kink velocity on the number N of cosine potentials for $\gamma = 0.5$ (top curves) and $\gamma = 0.2$ (bottom curves). The results obtained by using the collective coordinate theory are depicted with a solid line ($\gamma = 0.5$) and a dashed line ($\gamma = 0.2$). The results obtained from the simulations of the sG equation are plotted with circles ($\gamma = 0.5$) and triangles ($\gamma = 0.2$). The remaining parameter values are $\beta_j = 0.8$ for $j = 1, \ldots, N$.

to the potential $U_{j+1}(\Phi)$, which can be easily simulated by generating a set of random numbers z_j between 0 and 1, and assigning a residence time $\tau_j = -\ln(z_j)/\gamma$ to each potential state.

In this case, the symmetry condition (i) of Sec. II holds. If the permutation $\tilde{\sigma} j = N + 1 - j$ is applied, it clearly follows that

$$\theta_{\tilde{\sigma} j} = \frac{2\pi(j - N - 1)}{N} = -\frac{2\pi(N+1)}{N} + \frac{2\pi j}{N} = 2\bar{\theta} - \theta_j. \quad (37)$$

Additionally, condition (ii) is evidently fulfilled because all the frictions are equal. However, condition (iii) is broken since

$$W_{\tilde{\sigma} j, \tilde{\sigma} j'} = W_{N+1-j, N+1-j'} = \gamma \delta_{1-j, 2-j'} = \gamma \delta_{j, j'-1} \neq W_{j,j'}. \quad (38)$$

In Fig. 5, the averaged kink velocity is plotted vs the parameter N, for $\gamma = 0.5$ and $\gamma = 0.2$ (upper and lower curves, respectively). The most interesting feature of this figure is the high efficiency of the ratchet mechanism reflected in the large values of the resulting velocities. The excellent agreement between the CC theory (solid and dashed lines) and the simulations (circles and triangles) is also remarkable, especially for large values of N, that is, when transitions between potential states are sufficiently smooth. Note that even for those large values of N, the efficiency of the ratchet mechanism remains very high and the kink velocities are three orders of magnitudes over those obtained in Sec. III.

In order to better understand how this high efficiency is obtained, let us compare the two-state sG system considered at the beginning of Sec. III with the N-state sG system considered here. In the first case, the phase difference between two consecutive states of the process $\theta_{J(t)}$ alternately takes the values $\theta_2 - \theta_1$ and $\theta_1 - \theta_2$. Depending on whether this phase difference is positive or negative, the kink center moves backward or forward, respectively. The result is, therefore, a sequence of forward and backward displacements, as can be seen in Fig. 1. When $W_{1,2} \neq W_{2,1}$, these forward and backward displacements do not cancel each other, resulting in a nonzero net displacement of the kink but with a low average velocity. By contrast, in the N-state system, the phase difference between two consecutive states of $\theta_{J(t)}$ is always $-2\pi/N$ [note that a phase difference of $2\pi(N-1)/N$ is equivalent to a phase difference of $-2\pi/N$]. As a consequence, the kink center always moves forward, thus significantly improving the efficiency of the ratchet mechanism.

V. CONCLUSIONS

In this paper, a study of a type of stochastic soliton ratchet has been addressed. The generation of directed soliton motion is induced by random transitions among a set of symmetric sG potentials. These potentials are identical except for the presence of state-dependent phase shifts. In addition, each potential state has its own dissipation coefficient. Remarkably, in our study, neither thermal noise nor external forces are present.

A rigorous analysis of the symmetries of the stochastic system has been provided since, as is well known, the emergence of net motion is mainly determined by the breakdown of such symmetries. This analysis leads us to predict the necessary conditions for the existence of transport and for the appearance of current reversals upon the variation of the system parameters. By means of numerical simulations, various different ways of reaching net motion have been explored. The case of unequal transfer rates among the potential states has first been considered, but other possibilities, such as unequal frictions and suitable combinations of three (or more) symmetric sG states, have also been investigated.

As a consequence of this investigation, a very efficient soliton ratchet has been designed by means of properly tuning the random fluctuations among N symmetric sG potentials. It is to be expected that the high average velocities observed with this rectification mechanism will raise interest in the exploration of possible experimental research in this area. Moreover, although our study is restricted to sG-like equations, the results obtained can be extended to other models with topological soliton solutions.

ACKNOWLEDGMENTS

We acknowledge financial support from the Junta de Andalucía and from the Ministerio de Economía y Competitividad of Spain through Nos. FIS2017-86478-P (J.C.-P) and FIS2017-89349-P (N.R.Q.). N.R.Q. also acknowledges financial support from the Alexander von Humboldt Foundation and the hospitality of the Physikalisches Institut at the University of Bayreuth (Germany) during the completion of this work. This study has been partially financed by the Consejería de Conocimiento, Investigación y Universidad, Junta de Andalucía, and European Regional Development Fund (ERDF), Ref. No. SOMM17/6105/UGR.

APPENDIX: COLLECTIVE COORDINATE THEORY

Here, the same approach is used as that developed in Sec. III of Ref. 25 in order to obtain the equations of motion for the collective coordinates. To this end, let us propose a solution of Eqs. (1), (3), and (6) of the form $\Phi(x,t) = \Psi(x,t) + \varphi(t)$, where $\Psi(x,t)$ is the "naked" kink field, for which $\lim_{x\to-\infty}\Psi(x,t) = 0$. The background field is represented by $\varphi(t)$ and satisfies the differential equation

$$\ddot{\varphi}(t) = -\beta_{J(t)}\dot{\varphi}(t) - \sin\left[\varphi(t) + \theta_{J(t)}\right], \tag{A1}$$

with the initial conditions $\varphi(0) = -\bar{\theta}$ and $\dot{\varphi}(0) = 0$. Here, the dots denote the derivative with respect to time. For the function $\Phi(x,t)$, we use the same ansatz proposed in Ref. 25 with two collective coordinates, $X(t)$ and $L(t)$, which are, respectively, the center of mass and the width of the kinklike structure. Straightforward calculations of the time variation of the energy and the momentum of the kink (for details, see Ref. 25), yield the kink velocity

$$\dot{X}(t) = \frac{\pi L(t)\dot{\varphi}(t)}{4} \tag{A2}$$

and

$$\ddot{L}(t) = \frac{\left[\dot{L}(t)\right]^2}{2L(t)} - \frac{3L(t)\left[\dot{\varphi}(t)\right]^2}{8} - \beta_{J(t)}\dot{L}(t) + \frac{6}{\pi^2 L(t)}\left\{1 - \left[L(t)\right]^2\cos\left[\varphi(t) + \theta_{J(t)}\right]\right\}, \tag{A3}$$

which has to be solved with the initial conditions $L(0) = 1$ and $\dot{L}(0) = 0$.

Finally, the average kink velocity can be calculated from Eqs. (8) and (A2) after numerically solving the differential equations (A1) and (A3).

REFERENCES

[1] P. Reimann, "Brownian motors: Noisy transport far from equilibrium," Phys. Rep. **361**, 57 (2002).
[2] D. Cubero, J. Casado-Pascual, A. Alvarez, M. Morillo, and P. Hänggi, "Overdamped deterministic ratchets driven by multifrequency forces," Acta Phys. Pol. B **37**, 1467 (2006).
[3] P. Hänggi and F. Marchesoni, "Artificial brownian motors: Controlling transport on the nanoscale," Rev. Mod. Phys. **81**, 387 (2009).
[4] M. Salerno and N. R. Quintero, "Soliton ratchets," Phys. Rev. E **65**, 025602 (2002).
[5] A. V. Gorbach, S. Denisov, and S. Flach, "Optical ratchets with discrete cavity solitons," Opt. Lett. **31**, 1702 (2006).
[6] J. E. Villegas, S. Savel'ev, F. Nori, E. M. González, J. V. Anguita, R. García, and J. L. Vicent, "A superconducting reversible rectifier that controls the motion of magnetic flux quanta," Science **302**, 1188 (2003).
[7] A. V. Ustinov, C. Coqui, A. Kemp, Y. Zolotaryuk, and M. Salerno, "Ratchet-like dynamics of fluxons in annular Josephson junctions driven by biharmonic microwave fields," Phys. Rev. Lett. **93**, 087001 (2004).
[8] M. Beck, E. Goldobin, M. Neuhaus, M. Siegel, R. Kleiner, and D. Koelle, "High-efficiency deterministic Josephson vortex ratchet," Phys. Rev. Lett. **95**, 090603 (2005).
[9] D. Cole, S. Bending, S. Savel'ev, A. Grigorenko, T. Tamegai, and F. Nori, "Ratchet without spatial asymmetry for controlling the motion of magnetic flux quanta using time-asymmetric drives," Nat. Mater. **5**, 305 (2006).
[10] F. Martínez-Pedrero, P. Tierno, T. H. Johansen, and A. V. Straube, "Regulating wave front dynamics from the strongly discrete to the continuum limit in magnetically driven colloidal systems," Sci. Rep. **6**, 19932 (2016).
[11] J. Brox, P. Kiefer, M. Bujak, T. Schaetz, and H. Landa, "Spectroscopy and directed transport of topological solitons in crystals of trapped ions," Phys. Rev. Lett. **119**, 153602 (2017).
[12] E. Goldobin, D. Koelle, and R. Kleiner, "Tunable $\pm\varphi$, φ_0 and $\varphi_0 \pm \varphi$ Josephson junction," Phys. Rev. B **91**, 214511 (2015).
[13] J. A. Cuesta, N. R. Quintero, and R. Alvarez-Nodarse, "Time-shift invariance determines the functional shape of the current in dissipative rocking ratchets," Phys. Rev. X **3**, 041014 (2013).
[14] J. Casado-Pascual, J. A. Cuesta, N. R. Quintero, and R. Alvarez-Nodarse, "General approach for dealing with dynamical systems with spatiotemporal periodicities," Phys. Rev. E **91**, 022905 (2015).
[15] M. Schiavoni, L. Sánchez-Palencia, F. Renzoni, and G. Grynberg, "Phase control of directed diffusion in a symmetric optical lattice," Phys. Rev. Lett. **90**, 094101 (2003).
[16] S. Ooi, S. Savel'ev, M. B. Gaifullin, T. Mochiku, K. Hirata, and F. Nori, "Nonlinear nanodevices using magnetic flux quanta," Phys. Rev. Lett. **99**, 207003 (2007).
[17] A. V. Arzola, K. Volke-Sepulveda, and J. L. Mateos, "Experimental control of transport and current reversals in a deterministic optical rocking ratchet," Phys. Rev. Lett. **106**, 168104 (2011).
[18] S. Flach, Y. Zolotaryuk, A. E. Miroshnichenko, and M. V. Fistul, "Broken symmetries and directed collective energy transport in spatially extended systems," Phys. Rev. Lett. **88**, 184101 (2002).
[19] L. Morales-Molina, N. R. Quintero, F. G. Mertens, and A. Sánchez, "Internal mode mechanism for collective energy transport in extended systems," Phys. Rev. Lett. **91**, 234102 (2003).
[20] N. R. Quintero, B. Sánchez-Rey, and M. Salerno, "Analytical approach to soliton ratchets in asymmetric potentials," Phys. Rev. E **72**, 016610 (2005).
[21] L. Morales-Molina, F. G. Mertens, and A. Sánchez, "Ratchet behavior in nonlinear Klein-Gordon systems with pointlike inhomogeneities," Phys. Rev. E **72**, 016612 (2005).
[22] V. Berardi, J. Lydon, P. G. Kevrekidis, C. Daraio, and R. Carretero-González, "Directed ratchet transport in granular chains," Phys. Rev. E **88**, 052202 (2013).
[23] N. R. Quintero, "Soliton ratchets in sine-Gordon-like equations," in *The sine-Gordon Model and its Applications*, Nonlinear Systems and Complexity Vol. 10, edited by J. Cuevas-Maraver, P. Kevrekidis, and F. Williams (Springer, Cham, 2014).
[24] E. Zamora-Sillero, N. R. Quintero, and F. G. Mertens, "Ratchet effect in a damped sine-Gordon system with additive and parametric ac driving forces," Phys. Rev. E **74**, 046607 (2006).
[25] B. Sánchez-Rey, J. Casado-Pascual, and N. R. Quintero, "Kink ratchet induced by a time-dependent symmetric field potential," Phys. Rev. E **94**, 012221 (2016).
[26] C. Doering, "Stochastic ratchets," Physica A **254**, 1 (1998).

[27]M. O. Magnasco, "Forced thermal ratchets," Phys. Rev. Lett. **71**, 1477 (1993).
[28]R. D. Astumian, "Thermodynamics and kinetics of a Brownian motor," Science **276**, 917 (1997).
[29]P. Reimann and P. Hänggi, "Introduction to the physics of Brownian motors," Appl. Phys. A **75**, 169 (2002).
[30]M. Carusela, A. Fendrik, and L. Romanelli, "Transport and dynamical properties of inertial ratchets," Physica A **388**, 4017 (2009).
[31]A. J. Fendrik, L. Romanelli, and M. V. Reale, "Currents in defective coupled ratchets," Phys. Rev. E **85**, 041149 (2012).
[32]F. Marchesoni, "Thermal ratchets in 1+1 dimensions," Phys. Rev. Lett. **77**, 2364 (1996).
[33]A. V. Savin, G. P. Tsironis, and A. V. Zolotaryuk, "Reversal effects in stochastic kink dynamics," Phys. Rev. E **56**, 2457 (1997).
[34]M. Salerno and Y. Zolotaryuk, "Soliton ratchetlike dynamics by ac forces with harmonic mixing," Phys. Rev. E **65**, 056603 (2002).
[35]A. Sánchez, L. Morales-Molina, F. G. Mertens, N. R. Quintero, J. Buceta, and K. Lindenberg, "Ratchets in homogeneous extended systems: Internal modes and the role of noise," Fluct. Noise Lett. **4**, L571 (2004).
[36]Y. Zolotaryuk and M. Salerno, "Discrete soliton ratchets driven by biharmonic fields," Phys. Rev. E **73**, 066621 (2006).
[37]G. Carapella and G. Costabile, "Ratchet effect: Demonstration of a relativistic fluxon diode," Phys. Rev. Lett. **87**, 077002 (2001).
[38]F. Falo, P. J. Martínez, J. J. Mazo, T. P. Orlando, K. Segall, and E. Trías, "Fluxon ratchet potentials in superconducting circuits," Appl. Phys. A **75**, 263 (2002).
[39]J. Casado-Pascual, "Flux reversal in a simple random-walk model on a fluctuating symmetric lattice," Phys. Rev. E **74**, 021112 (2006).
[40]H. Hagman, M. Zelan, and C. M. Dion, "Breaking the symmetry of a Brownian motor with symmetric potentials," J. Phys. A Math. Theor. **44**, 155002 (2011).
[41]Z. Gui-Chuan and L. Jing-Hui, "Effect of asymmetry of dichotomous noise on transport of particles," Commun. Theor. Phys. **53**, 303 (2010).
[42]R. Kanada and K. Sasaki, "Thermal ratchets with symmetric potentials," J. Phys. Soc. Jpn. **68**, 3759 (1999).
[43]H. Susanto, "Localized modes and phonon scattering of a lattice κ kink," Phys. Rev. E **73**, 026608 (2006).
[44]Q. Liang, Y. Yu, Q. Wang, and J. Dong, "Controllable 0-π transition in a superconducting graphene-nanoribbon junction," Phys. Rev. Lett. **101**, 187002 (2008).
[45]D. B. Szombati, S. Nadj-Perge, D. Car, S. R. Plissard, E. P. A. M. Bakkers, and L. P. Kouwenhoven, "Josephson ϕ_0-junction in nanowire quantum dots," Nat. Phys. **12**, 568 (2016).
[46]S. von Gehlen, M. Evstigneev, and P. Reimann, "Ratchet effect of a dimer with broken friction symmetry in a symmetric potential," Phys. Rev. E **79**, 031114 (2009).
[47]J. Casado-Pascual, "Directed motion of spheres induced by unbiased driving forces in viscous fluids beyond the Stokes' law regime," Phys. Rev. E **97**, 032219 (2018).
[48]E. Goldobin, R. Menditto, D. Koelle, and R. Kleiner, "Model I–V curves and figures of merit of underdamped deterministic Josephson ratchets," Phys. Rev. E **94**, 032203 (2016).